



HAL
open science

Intraspecific variability in cardinal growth temperatures and water activities within a large diversity of *Penicillium roqueforti* strains

Karim Rigalma

► **To cite this version:**

Karim Rigalma. Intraspecific variability in cardinal growth temperatures and water activities within a large diversity of *Penicillium roqueforti* strains. *Food Research International*, 2021, 148, pp.110610. 10.1016/j.foodres.2021.110610 . hal-03736420

HAL Id: hal-03736420

<https://hal.inrae.fr/hal-03736420>

Submitted on 22 Aug 2023

HAL is a multi-disciplinary open access archive for the deposit and dissemination of scientific research documents, whether they are published or not. The documents may come from teaching and research institutions in France or abroad, or from public or private research centers.

L'archive ouverte pluridisciplinaire **HAL**, est destinée au dépôt et à la diffusion de documents scientifiques de niveau recherche, publiés ou non, émanant des établissements d'enseignement et de recherche français ou étrangers, des laboratoires publics ou privés.



Distributed under a Creative Commons Attribution - NonCommercial 4.0 International License

1 **Intraspecific variability in cardinal growth temperatures and water activities within a**
2 **large diversity of *Penicillium roqueforti* strains**

3

4 Nicolas Nguyen Van Long^{1*}, Karim Rigalma¹, Jean-Luc Jany¹, Jérôme Mounier¹, Valérie
5 Vasseur¹

6

7 ¹Université de Brest, EA 3882, Laboratoire Universitaire de Biodiversité et Ecologie
8 Microbienne, IBSAM, ESIAB, Technopôle Brest-Iroise, 29280 Plouzané, France

9 *Present address: ADRIA Food Technology Institute, ZA Creac'h Gwenn, 29000 Quimper,
10 France.

11

12 **Keywords**

13 Predictive mycology; Intraspecific variability; Temperature; Water activity; Fungal radial
14 growth; *Penicillium roqueforti*

15

16 **Highlights**

- 17 • Minimal and optimal growth temperatures of *Penicillium roqueforti* were associated
18 with an important intraspecific variability.
- 19 • Cardinal a_w values were associated with lower intraspecific variability in comparison
20 to cardinal temperatures

21

22 **Abstract**

23 Different strains of a given fungal species may display heterogeneous growth behavior in
24 response to environmental factors. In predictive mycology, the consideration of such
25 variability during data collection could improve the robustness of predictive models. Among

26 food-borne fungi, *Penicillium roqueforti* is a major food spoiler species which is also used as
27 a ripening culture for blue cheese manufacturing. In the present study, we investigated the
28 intraspecific variability of cardinal temperatures and water activities (a_w), namely, minimal
29 (T_{min} and a_{wmin}), optimal (T_{opt} and a_{wopt}) and maximal (T_{max}) temperatures and/or a_w estimated
30 with the cardinal model for radial growth, of 29 *Penicillium roqueforti* strains belonging to 3
31 genetically distinct populations. The mean values of cardinal temperatures and a_w for radial
32 growth varied significantly across the tested strains, except for T_{max} which was constant. In
33 addition, the relationship between the intraspecific variability of the biological response to
34 temperature and a_w and putative genetic populations (based on microsatellite markers) within
35 the selected *P. roqueforti* strains was investigated. Even though no clear relationship was
36 identified between growth parameters and ecological characteristics, PCA confirmed that
37 certain strains had marginal growth response to temperature or a_w . Overall, the present data
38 support the idea that a better knowledge of the response to abiotic factors such as temperature
39 and a_w at an intraspecific level would be useful to model fungal growth in predictive
40 mycology approaches.

41

42 **1. Introduction**

43 Fungal spoilage of food and feed are responsible for important economic losses (Legan, 1993)
44 and may be responsible for food safety issues, depending on the ability of certain fungal taxa
45 to produce mycotoxins (García et al., 2009). Fungal growth in food and feed can be affected
46 by environmental factors, including intrinsic and extrinsic parameters. Water activity (a_w),
47 pH, texture, available nutrients and antimicrobial substances are the main intrinsic factors,
48 while temperature, humidity and atmosphere composition of the storage environment are the
49 main extrinsic factors.

50 The combination of these factors, also called the hurdle technology concept, represents an
51 effective tool for food safety and quality management (Leistner and Gorris, 1995). In the case
52 of fungi, predictive mycology approach can be used to study the influence of such hurdles on
53 biological responses including spore germination, mycelial growth or mycotoxin production
54 (Valík et al., 1999; Dantigny et al., 2005; Delhalle et al., 2012; Leggieri et al., 2017). In
55 predictive mycology, kinetic parameters are generally studied on culture media as a function
56 of environmental factors in order to determine cardinal values, namely minimal, optimal and
57 maximal values (Dagnas and Membré, 2013). These specific cardinal values can then be used
58 to predict fungal growth in food and feed as a function of the prevailing environmental
59 conditions.

60

61 As reviewed by García et al (2012), *in vitro* experiments are generally performed with a
62 limited number of fungal strains for each studied species. Indeed, out of 127 published studies
63 between 2000 and 2010, the mean number of strains/species was lower than 3, which is
64 relatively low when considering the intraspecific diversity of fungi encountered in food and
65 feed. Yet, using a collection of 62 *Penicillium expansum* and 30 *Aspergillus carbonarius*
66 isolates, García et al (2012) demonstrated that growth kinetic parameters varied at the
67 intraspecies level and that a minimum number of strains needed to be studied in order to
68 correctly reflect the intraspecific variability of these parameters. This minimum number was
69 of 25-30 and 12-17 strains for *P. expansum* and *A. carbonarius*, respectively (García et al.,
70 2012). Moreover, as shown previously for *Penicillium roqueforti*, an intraspecific variability
71 in morphological traits (Gillot et al., 2015), proteolytic activity (Gillot et al., 2016) or the
72 ability to produce mycotoxins (Aldars-García et al., 2018a; Fontaine et al., 2015) also exists
73 within fungal species. In natural ecosystems as well as food products, different strains of a
74 same species can occupy the same niche (Aldars-García et al., 2018a), it is thus questionable

75 whether growth predictions based on a limited number of strains could be representative of
76 the behavior of fungal spoilers in a food spoilage situation.

77

78 *Penicillium roqueforti* is a major spoiler in foods including dairy products (Garnier et al.,
79 2017) and is also used as a ripening culture in blue-cheese production (Cantor et al., 2004). In
80 a previous study (Gillot et al., 2015) the morphological and genetic diversity among a
81 worldwide collection of 164 *P. roqueforti* was explored. A high level of macro-
82 morphological diversity was highlighted regarding colors and textures of the mycelia as well
83 as in the size of the colony margin. Using 4 microsatellite markers, 28 different haplotypes
84 were identified and these haplotypes were distributed into three highly differentiated genetic
85 populations (Gillot et al., 2015). Using well-characterized strains selected from the
86 aforementioned study as biological models, the present study aimed at exploring the
87 intraspecific variability in cardinal temperatures and a_w for radial growth of *P. roqueforti*. The
88 respective effects of temperature and a_w on fungal growth were studied following two
89 independent monofactorial experimental designs.

90

91 **2. Material and methods**

92 **2.1 Fungal strains**

93 Twenty-nine *P. roqueforti* strains isolated from cheese and various environments were
94 studied (Table 1). Among them, 28 strains were previously characterized at the genetic level
95 by Gillot et al. (2015). Each one of them represented a different haplotype and belonged to 3
96 genetically highly differentiated populations, as determined by Gillot et al. (2015). An
97 additional *P. roqueforti* strain (B20) was also included. The latter strain was previously used
98 in predictive mycology studies (Nguyen Van Long et al., 2017a; 2017b), and found to belong
99 to genetic population 2 according to populations described by Gillot et al. (2015). For the

100 present study, strain codes were used (A = genetic population 1, B = genetic population 2 and
101 C = genetic population 3). These 29 fungal strains were routinely cultured on potato dextrose
102 agar (PDA, potato extract 4g/L, dextrose 20g/L, agar 15g/L, Difco, Becton Dickinson, Sparks,
103 MD, USA) at 25 °C.

104

105 **2.2 Experimental design**

106 The respective effects of both temperature and a_w factors were studied independently by the
107 means of monofactorial experimental designs for which the levels of unstudied factors were
108 fixed at arbitrary levels (25 °C and 0.980). For temperature experiments, ten temperature
109 levels were tested, *i.e.*, 2, 5, 7, 10, 20, 22, 25, 27, 30 and 32 °C. These temperature levels
110 were selected in order to better target theoretical minimal, optimal and maximal temperatures
111 in a limited number of experiments. For example, no additional temperature was tested
112 between 10 °C and 20 °C because it was not required for modelling purpose. For a_w
113 experiments, six a_w levels (0.830, 0.853, 0.898, 0.943, 0.965, 0.995) were obtained by using
114 sodium chloride (NaCl) at a final concentration ranging from 0 to 14.5 % (w/w). This a_w -
115 depressor was chosen on the basis of previous experiments (Nguyen Van Long et al., 2017a)
116 and in order to better represent environmental conditions that fungi can encounter in foods.

117

118 **2.3 Culture media**

119 The culture medium used throughout this study was PDA supplemented with a 3:2 (v/v)
120 mixture of citric acid monohydrate (0.1 M) and dibasic sodium phosphate (0.2 M) solutions
121 (Sigma-Aldrich, Saint-Louis, MO, USA) in order to set the pH level at 4.2. The a_w -depressor
122 solutions and double concentrated agar medium were prepared and autoclaved separately
123 before mixing and pouring 25 mL into 90-mm Petri dishes. For each batch of culture medium,
124 pH and a_w were checked in three replicates at 20 °C using a pH surface-electrode (SF 113,

125 VWR, Radnor, PA, USA) with an accuracy of 0.01 pH unit and an a_w -meter (Tunable Diode
126 Laser a_w -meter Aqualab, Decagon Devices, Pullman, WA, USA) with an accuracy of 0.005
127 a_w unit. The a_w apparatus was calibrated according to the manufacturer's instructions using
128 salt solutions of known a_w .

129

130 **2.4 Conidia production**

131 Conidia were harvested from cultures incubated for 10 days at 25 °C on PDA medium at
132 0.980 a_w and pH 4.2. For temperature experiments, the conidia harvesting solution was a
133 glycerol solution adjusted to 0.980 a_w containing Tween 80 (0.01 % v/v). For a_w experiments,
134 the conidia were harvested in different buffered NaCl solutions with a_w values corresponding
135 to the different culture media (pH = 4.20). Conidial concentrations were determined using a
136 haemocytometer (Malassez, Preciss, Paris, France) and diluted using the same glycerol or
137 NaCl solutions to obtain a 1.10^6 conidia/mL suspension prior to inoculation.

138

139 **2.5 Radial growth assessment**

140 Ten microliters of the conidia suspension were deposited in the center of agar plates. These
141 plates were then placed in plastic boxes (34x25x12 cm) containing 200 mL of NaCl solution
142 adjusted to the corresponding a_w of the culture medium in order to avoid a_w fluctuation
143 (Sautour et al., 2001) and incubated in temperature-controlled incubators (KB 240, Binder
144 GmbH, Tuttlingen, Germany). Thallus diameter was measured daily in 2 perpendicular
145 directions for a maximum of 60 days and the mean radius calculated based on data from 4
146 biological replicates.

147

148 **2.6 Data modelling and statistical analysis**

149 **2.6.1 Primary modelling of radial growth kinetics**

150 Radial growth was described as a function of incubation time with the logistic model with
 151 latency and breaking adapted to the radial growth of filamentous fungi (Augustin and Carlier,
 152 2000; Rosso, 1995) (Eq. 1):

153

$$154 \quad r(t) = \begin{cases} r_0, & t \leq \lambda \\ \ln(r_{max}) - \ln\left(1 + \left(\frac{r_{max}}{r_0} - 1\right) \cdot e^{-\mu \cdot (t-\lambda)}\right), & t > \lambda \end{cases} \quad (\text{Eq. 1})$$

155

156 where $r(t)$ is the radius of the thallus (mm) at the time of incubation t (d), λ is the latency (d)
 157 before growth characterized by μ , the radial growth rate (mm.d⁻¹) and r_{max} is the maximum
 158 radius (mm) of the thallus over incubation time. In the present study, the radius r_0 was fixed
 159 at 3 mm, corresponding to the diameter of the inoculum. The model was fitted by minimizing
 160 the sum of squares of the residuals (*lsqcurvefit* function, Matlab 2014 The Mathworks Inc.,
 161 USA). Estimated parameter confidence intervals of 95% were calculated with traditional
 162 methods based on a linear approximation (*nlrparci* function of Matlab, at 95% of confidence).
 163 The model fitting performances were evaluated using the determination coefficient (r^2) and
 164 the root mean square error (RMSE).

165

166 **2.6.2 Secondary modelling of radial growth rate and latency as a function of** 167 **temperature or a_w**

168 The parameters λ and μ were independently modelled as a function of the temperature or a_w
 169 levels. The radial growth rate (μ) was modelled as a function of both factors with cardinal
 170 model, described by Eq. 2 (Rosso et al., 1995):

171

$$172 \quad \sqrt{\mu} = \sqrt{\mu_{opt} \cdot CM_2(T) \cdot CM_2(a_w)}$$

173 $CM_n(X)$

$$174 = \begin{cases} 0 & X \leq X_{min} \\ \frac{(X-X_{max}) \cdot (X-X_{min})^n}{(X_{opt}-X_{min})^{n-1} \cdot \{(X_{opt}-X_{min}) \cdot (X-X_{opt}) - (X_{opt}-X_{max})[(n-1) \cdot X_{opt} + X_{min} - n \cdot X]\}}, & X_{min} < X < X_{max} \\ 0 & X \geq X_{max} \end{cases} \quad (\text{Eq. 2})$$

175

176 where X_{min} , X_{opt} and X_{max} (cardinal temperature or a_w values) are respectively the minimum,
 177 optimum and maximum temperature or a_w values (a_{wmax} is considered as a constant = 1), n is a
 178 shape parameter ($n = 2$ in temperature and a_w experiments), μ is the radial growth rate and
 179 μ_{opt} the value of μ when $T = T_{opt}$ or when $a_w = a_{wopt}$, namely the optimal radial growth rate.
 180 The reciprocal of latency for radial growth (λ^{-1}) was modelled as a function of temperature
 181 with Eq. 2 where μ was substituted by λ^{-1} and μ_{opt} was substituted by λ^{-1}_{opt} , namely the value
 182 of λ^{-1} when $T = T_{opt}$ or $a_w = a_{wopt}$. The models were fitted by minimizing the sum of squares of
 183 the residuals (*lsqcurvefit function*, Matlab 2014 The Mathworks Inc., USA). The fitting were
 184 performed independently for four biological replicates. Estimated parameter confidence
 185 intervals at 95% and model fitting performances were determined as described above.

186

187

188 **2.6.4 Statistical analysis**

189 Mean values of secondary modelling parameters (namely cardinal temperatures, cardinal a_w ,
 190 μ_{opt} and λ^{-1}_{opt}) obtained with 4 biological replicates/strain were used to describe the variability
 191 among the different *P. roqueforti* strains by means of box plots (*boxplot* function of Matlab).
 192 The box plots allowed to display descriptive statistics such as the median value, the 25th and
 193 75th percentiles, minimal and maximal values as well as outliers. Skewness was calculated
 194 using *skewness* function of Matlab. Strains were considered as outlier when their value for a
 195 given parameter was at least 1.5 times the interquartile range away from the box (either top or
 196 bottom). When outliers were observed, their respective sets of parameters were compared to
 197 that of any other strain by means of one-vs-one likelihood ratio test (LRT; Huet et al., 2004;

198 Morin-Sardin et al., 2016; Nguyen Van Long et al., 2017b). First, for a given couple of strains
199 to be compared, the model was fitted independently to estimate model parameters for each
200 strain (unconstrained model, U). Secondly, a new fit was performed in the case where the
201 value of one parameter was hypothesized to be equal for both strains (constrained model, C).
202 Fits of U and C models were compared using the statistic SL , defined as (Eq. 3):

203

$$204 \quad SL = n \cdot \log(RSS_C) - n \cdot \log(RSS_U) \quad (3)$$

205

206 where n is the length of data set, RSS_C and RSS_U are the residual square sum for the
207 constrained (C) and unconstrained (U) model respectively. When n tends to infinity, the
208 limiting distribution of SL is a Chi-square test (Chi^2) distributed with a degree of freedom
209 equal to the number of constrained parameters. When $SL \leq \text{Chi}^2$ ($\alpha = 0.05$), the difference of
210 fit between both models is considered significant, indicating that growth behavior of both
211 strains cannot be described by the same secondary modelling parameters.

212

213 In order to investigate the correlations between the different parameters, a principal
214 component analysis (PCA) was performed with the *pca* function of Matlab.

215

216 **3. Results**

217 **3.1 Primary modelling of radial growth kinetics**

218 Growth of the 29 *P. roqueforti* strains was observed at temperatures ranging from 2 °C to 30
219 °C and a_w ranging from 0.995 to 0.850 (0.0 % to 12.7 % NaCl w/w). Noteworthy, no growth
220 was observed at 0.830 a_w nor at 32 °C within the 60-days incubation period. Independently of
221 the tested strains and culture conditions, radial growth kinetics were characterized by a lag
222 phase (during which the thallus diameter was inferior to that of the inoculum diameter),

223 followed by a linear phase of radial growth. The primary model (Eq. 1) was able to describe
224 radial growth with a satisfying fitting quality as reflected by r^2 calculated above 0.80 and
225 RMSE calculated below 5.32 mm (Supplementary table 1). In certain conditions, fungal
226 growth stopped before the end of incubation time (60 days) and thus did not reach the side
227 borders of the Petri dish. In this condition, the thallus radius at the end of incubation time was
228 estimated by the r_{max} parameter (Eq. 1). Otherwise, the r_{max} parameter equals the diameter of
229 the Petri dish. As the r_{max} parameter is not a kinetic parameter and can be related to the Petri
230 dish size, it was not used for secondary modelling.

231

232 **3.2 Effect of temperature and a_w on latency for radial growth**

233 Both incubation temperature and a_w affected the latency for growth parameter λ (Fig. 1 and
234 Fig. 2). Concerning the incubation temperature, two different types of responses were
235 observed. For 11 strains (A1, A2, A3, B1, B2, B3, B9, B13, B15, C1 and C3) latency
236 decreased (so λ^{-1} increased) as the temperature increased from 2 °C to 30 °C but no decrease
237 of λ^{-1} was observed at temperatures higher than the optimal level. In contrast, for the 18 other
238 strains, λ decreased as the temperature increased from 2 °C to a strain-dependent threshold,
239 and then increased at higher temperatures. The same two types of response were observed for
240 the a_w factor. For a minority of strains (A3, A4, A5, B1, B3, B4, B7 and B19), it was possible
241 to observe an a_w level for which the λ^{-1} was higher than its value at 0.995 a_w . In contrast for
242 the 21 other strains, no increase of λ^{-1} (compared to its level at 0.995 a_w) was observed in the
243 tested a_w range. The cardinal model (Eq. 2) was able to describe the effect of temperature and
244 a_w within the tested ranges on λ^{-1} with r^2 values higher than or equal to 0.703 and RMSE
245 lower than or equal to 0.161 d⁻¹ (Table 2). The cardinal model provided six parameters
246 describing the effect of temperature and a_w on the latency for radial growth for each strain: the

247 minimal (T_{min}), optimal (T_{opt}) and maximal (T_{max}) temperatures, the minimal (a_{wmin}) and
248 optimal (a_{wopt}) a_w and the value of λ^{-1} under optimal temperature and a_w namely, λ^{-1}_{opt} .

249

250 **3.3 Effect of temperature and a_w on radial growth rate**

251 Both incubation temperature and a_w affected the radial growth rate parameter (Fig. 3 and Fig.
252 4). Concerning the incubation temperature, the same type of response was observed for all
253 strains: the μ parameter increased as the temperature increased from 2 °C to a certain strain-
254 dependent threshold, and then decreased at higher temperatures. For the a_w factor, two
255 different types of responses were observed. For 14 strains (A2, B1, B2, B3, B4, B7, B10,
256 B11, B12, B13, B14, B15, B17 and B19) , μ decreased as the a_w decreased from 0.995 to
257 0.850 and no increase of λ^{-1} (compared to its level at 0.995 a_w) was observed in the tested a_w
258 range. In contrast for the 15 other strains, μ increased as the a_w decreased from 0.995 to a
259 strain-dependent threshold, and then decreased at lower a_w levels. The cardinal model (Eq. 2)
260 was able to describe the effect of temperature and a_w within the tested ranges on μ with r^2
261 values higher than or equal to 0.808 and RMSE lower than or equal to 0.334 mm.d⁻¹ (Table
262 3). The cardinal model provided six parameters describing the effect of temperature and a_w on
263 radial growth rate: the minimal (T_{min}), optimal (T_{opt}) and maximal (T_{max}) temperatures, the
264 minimal (a_{wmin}) and optimal (a_{wopt}) a_w and the value of μ under optimal temperature and a_w
265 namely, μ_{opt} .

266 **3.4 Intraspecific variability in secondary modelling parameters**

267 **3.4.1 Intraspecific variability in secondary modelling temperature and a_w parameters** 268 **for latency for radial growth**

269 The temperature-related parameters varied significantly at the intra-species level as illustrated
270 by the boxplot figures (Fig. 5). The distribution of T_{min} was positively skewed (skewness =
271 0.478) and ranged between -12.8 °C ± 0.4 °C (strain A3) and -2.1 °C ± 0.2 °C (strain B11)

272 with a median of $-8.4\text{ }^{\circ}\text{C}$ and a difference of $4.0\text{ }^{\circ}\text{C}$ between the 25th and 75th percentiles. The
273 distribution of T_{opt} was relatively symmetric (skewness = 0.053) and ranged between $21.5\text{ }^{\circ}\text{C}$
274 $\pm 0.5\text{ }^{\circ}\text{C}$ (strain B11) and $35.3\text{ }^{\circ}\text{C} \pm 0.3\text{ }^{\circ}\text{C}$ (strain A1) with a median of $27.2\text{ }^{\circ}\text{C}$ and a
275 difference of $4.7\text{ }^{\circ}\text{C}$ between the 25th and 75th percentiles. The distribution of T_{max} was also
276 relatively symmetric (skewness = 0.041) and ranged between $27.0\text{ }^{\circ}\text{C} \pm 0.01\text{ }^{\circ}\text{C}$ (strains C1
277 and C2) and $35.3\text{ }^{\circ}\text{C} \pm 0.3\text{ }^{\circ}\text{C}$ (strain A1) with a median at $30.4\text{ }^{\circ}\text{C}$. It was narrower than the
278 two previous distributions with a difference of only $1.8\text{ }^{\circ}\text{C}$ between the 25th and 75th
279 percentiles. No outlier strain was observed in the boxplot figure for T_{min} and T_{opt} but 3 outlier
280 strains were identified for T_{max} (A1, C1 and C2). According to the LRT comparison versus 28
281 other strains, A1, C1 and C2 had significantly different T_{max} values from those of the other 20,
282 25 and 22 strains, respectively.

283 The a_w -related parameters also varied significantly at the intra-species level as illustrated by
284 the boxplot figures (Fig. 5). The distribution of a_{wmin} was negatively skewed (skewness = -
285 1.163) and ranged between 0.646 ± 0.076 (strain B19) and 0.810 ± 0.002 (strain A3) with a
286 median of 0.764 and a difference of 0.037 a_w unit between the 25th and 75th percentiles. The
287 distribution of a_{wopt} was also negatively skewed (skewness = -0.282) and ranged between
288 0.976 ± 0.001 (strain B7) and 0.998 ± 0.002 (strain B5) with a median of 0.988. It was
289 narrower than the previous distribution with a difference of 0.006 a_w unit between the 25th and
290 75th percentiles. No outlier strain was observed in the boxplot figure for a_{wopt} but 2 outlier
291 strains were identified for a_{wmin} (B5 and B19). According to the LRT comparison versus 28
292 other strains, B5 and B19 had significantly different a_{wmin} values from those of the other 20
293 and 24 strains, respectively.

294 The λ_{opt}^{-1} parameter was not highly variable at the intra-species level (Fig. 5). Its distribution
295 was positively skewed (skewness = 0.488) and ranged between $0.69\text{ d}^{-1} \pm 0.01\text{ d}^{-1}$ (strain B9)
296 and $1.17\text{ d}^{-1} \pm 0.02\text{ d}^{-1}$ (strain B6) with a median of 0.86 d^{-1} and a difference of 0.15 d^{-1}

297 between the 25th and 75th percentiles. No outlier strain was observed in the boxplot figure for
298 this parameter.

299

300 **3.4.2 Intraspecific variability in secondary modelling temperature and a_w parameters** 301 **for radial growth rate**

302 The temperature-related parameters varied significantly at the intra-species level as illustrated
303 by the boxplot figures (Fig. 5). The distribution of T_{min} was negatively skewed (skewness = -
304 0.887) and ranged between $-35.4\text{ °C} \pm 3.9\text{ °C}$ (strain B14) and $-8.8\text{ °C} \pm 0.5\text{ °C}$ (strain B17)
305 with a median of -16.4 °C and a difference of 7.9 °C between the 25th and 75th percentiles.
306 The distribution of T_{opt} was positively skewed (skewness = 0.503) and ranged between 22.5
307 $\text{°C} \pm 0.5\text{ °C}$ (strain B19) and $28.5\text{ °C} \pm 3.0\text{ °C}$ (strain B5) with a median of 24.8 °C and a
308 difference of 2.6 °C between the 25th and 75th percentiles. The distribution of T_{max} was
309 negatively skewed (skewness = -4,389) and ranged between $29.1\text{ °C} \pm 1.7\text{ °C}$ (strain B14) and
310 $30.3\text{ °C} \pm 0.1\text{ °C}$ (strain C4) with a median of 30.16 °C . It was narrower than the two previous
311 distributions with a difference of only 0.12 °C between the 25th and 75th percentiles. No
312 outlier strain was observed in the boxplot figure for T_{opt} but B14 was identified as an outlier
313 for both T_{min} and T_{max} . According to the LRT comparison versus 28 other strains, B14 had
314 T_{min} and T_{max} values significantly different from those of 25 and 15 strains, respectively.

315

316 The a_w -related parameters also varied significantly at the intra-species level as illustrated by
317 the boxplot figures (Fig. 5). The distribution of a_{wmin} was negatively skewed (skewness = -
318 1.754) and ranged between 0.753 ± 0.012 (strain B16) and 0.855 ± 0.017 (strain B10) with a
319 median of 0.832 and a difference of $0.023\ a_w$ unit between the 25th and 75th percentiles. The
320 distribution of a_{wopt} was positively skewed (skewness = 1.422) and ranged between $0.981 \pm$
321 0.002 (strain B8) and 1.032 ± 0.006 (strain B14) with a median of 0.987 . It was slightly

322 narrower than the previous distribution with a difference of 0.019 a_w unit between the 25th and
323 75th percentiles. The strains B16 and B14 were identified as outliers for a_{wmin} and a_{wopt} ,
324 respectively. According to the LRT comparison versus 28 other strains, B16 had a
325 significantly different a_{wmin} value from that of 26 strains and B14 had a significantly different
326 a_{wopt} value from that of the other 27 strains.

327 The μ_{opt} parameter was also variable at the intra-species level (Fig. 5). The distribution of μ_{opt}
328 was slightly negatively skewed (skewness = -0.258) and ranged between $3.34 \text{ mm.d}^{-1} \pm 0.27$
329 mm.d^{-1} (strain B14) and $7.01 \text{ mm.d}^{-1} \pm 0.13 \text{ mm.d}^{-1}$ (strain B3) with a median of 5.44 mm.d^{-1}
330 and a difference of 1.3 mm.d^{-1} between the 25th and 75th percentiles. No outlier strain was
331 observed in the boxplot figure for μ_{opt} .

332

333 **3.5 Principal component analysis**

334 The results of principal component analysis (PCA) are presented in Fig. 6. Overall, neither
335 clear clusters, nor specific distribution with regards to genetic populations or cheese *versus*
336 non-cheese substrate of origin were observed. Nonetheless, principal components 1 and 2
337 explained more than 57% (36.80 % and 20.74 % respectively) of the total variance. Position
338 of variables in the plane indicated that T_{min} , a_{wmin} and μ_{opt} had close coordinates in the plane
339 (data not shown). T_{min} (λ) appeared to be correlated in the first dimension with T_{min} (μ) and
340 μ_{opt} . The parameter λ^{-1}_{opt} appeared to be correlated to a_{wopt} (λ) in the second dimension. The
341 position of individuals in the plane showed that the growth behavior of some *P. roqueforti*
342 strains could be described by the two principal components (e.g., B14, A1, B10 and B5),
343 whereas some other strains were poorly described (e.g., C2). Noteworthy, some individuals
344 were positively (e.g., B10, B17) or negatively (e.g., B14, B16, B18) correlated to the group of
345 variables T_{min} (μ), a_{wmin} (μ) and μ_{opt} .

346

347 **4. Discussion**

348 In the present study, we investigated the intraspecific variability associated to cardinal
349 temperature and a_w values for radial growth of 29 *P. roqueforti* strains isolated from diverse
350 origins. As both radial growth kinetic parameters λ and μ were affected by the incubation
351 temperature and medium a_w , they were independently modelled as a function of both factors
352 with a cardinal model in order to obtain secondary modelling parameters, including cardinal
353 temperatures (T_{min} , T_{opt} and T_{max}) and a_w (a_{wmin} and a_{wopt}). These secondary modelling
354 parameters can be used for radial growth prediction of *P. roqueforti* on PDA medium with
355 specific regards to its biological variability. The present work also provided optimum growth
356 rate (μ_{opt}) and minimum lag time (λ^{-1}_{opt}) for PDA medium. Nevertheless, in order to make
357 predictions for specific food items, a food matrix validation would be required considering
358 that μ_{opt} and λ^{-1}_{opt} are considered to be food specific (Pinon et al., 2004).

359

360 In the present study, several cardinal values were outside the tested ranges of temperature or
361 a_w . It is important to consider these parameters as extreme levels estimated by the
362 mathematical models and not as observed growth limits (Ross et al., 2011). Therefore, they
363 can only be used to predict radial growth within the tested ranges of temperature and a_w and
364 any prediction outside these ranges would not be supported by observed data. For example,
365 all estimated T_{min} were negative values. The lowest tested temperature in the present work
366 was 2 °C at which all *P. roqueforti* strains showed visible radial growth. Further experiment
367 was performed in order to confirm the inability of B14 strain (lowest estimated T_{min}) to grow
368 at negative temperature (-20 °C) and no visible growth was observed after incubation for 90
369 days (data not shown). This demonstrates that outside the tested range, the current secondary
370 model is ineffective to describe temperature effect on *P. roqueforti*. However, the present
371 work confirms the psychrotolerance of this species, as previously reported elsewhere

372 (Cuppers et al., 1997; Saccomori et al., 2015). Further investigations are needed to propose
373 models for negative temperatures at which water freezing in culture media or food can lead to
374 a reduction of water availability hence representing an additional hurdle to fungal growth
375 (Gill and Lowry, 1982).

376 Interestingly, estimated T_{max} values characterizing temperature effect on λ^{-1} were mostly
377 above 30 °C although this temperature drastically inhibited mycelial growth. Because an
378 accurate estimation of T_{max} requires observation of a significant decrease of the kinetic
379 parameter above a certain threshold (which was not observed for λ^{-1} for several strains), the
380 cardinal model provided T_{max} values for the latency parameter which were not related to the
381 upper temperature limit for growth. Moreover, the absence of an observed decrease in λ^{-1} (or
382 increase of λ) at 30 °C can be explained by the fact that, for several strains, a thallus was
383 rapidly visible within the first days of incubation but this thallus then grew slowly ($\mu \leq 1.28$
384 mm.day⁻¹). This observation suggests that conidial germination could be less affected by a
385 temperature increase around T_{max} than hyphal elongation as latency for radial growth is
386 strongly linked to the germination process (Gougouli and Koutsoumanis, 2013). This could
387 occur in conditions allowing the conidial germination but inhibiting further hyphal extension.
388 It has been previously observed that under stressful conditions (extreme a_w levels),
389 *Aspergillus penicillioides* conidia started to germinate but did not produce visible mycelium
390 (Stevenson et al., 2017). Finally, there was in general a good agreement between cardinal
391 temperatures for latency and those for growth as previously reported for a large number of
392 fungal species (Gougouli et al., 2011).

393

394 As shown in previous studies (Araujo and Rodrigues, 2004; García et al., 2011a; Perneel et
395 al., 2006; Vidal et al., 1997; Walther et al., 2013), the present data confirmed that the growth
396 behavior of fungi, in this case *P. roqueforti*, can significantly vary at an intraspecies level, and

397 that a higher level of variability in biological response was observed in marginal
398 environmental conditions (Aldars-García et al., 2018a; 2018b). Biological responses other
399 than conidial germination and radial growth such as ascospore heat-resistance (Santos et al.,
400 2018) or conidia ethanol resistance (Visconti et al., 2020) can also vary at the intraspecific
401 level and subsequently be of importance to consider in predictive mycology. In temperature
402 experiments, both T_{min} and T_{opt} parameters showed the largest ranges, indicating that these
403 cardinal temperatures are characterized by a wider intraspecific variability whereas T_{max} was
404 almost constant for μ or slightly variable for λ . Accordingly, we can hypothesize based on the
405 present study (29 studied strains) that a temperature close to 30 °C is a growth limit in *P.*
406 *roqueforti* whereas the ability to produce a mycelium at refrigeration temperatures could be
407 highly strain-dependent.

408 Overall, the present results support the existence of an important intraspecific variability for
409 *P. roqueforti* cardinal temperatures and, to a lesser extent, for cardinal a_w . Such results
410 contrast with those of García et al. (2011b) on *Aspergillus carbonarius* for which a higher
411 intraspecific variability in growth response to a_w than temperature was found. LRT also
412 allowed us to evaluate if one secondary model parameter for a given strain can be substituted
413 by that of another strain without significant effect on the fitting quality. According to the
414 present results, it is possible to assume that several strains could not reasonably share the
415 same values of T_{min} , T_{max} or a_{wmin} .

416

417 In the present study, in order to understand the origin of this observed variability, a PCA was
418 carried out. Despite a low overall ratio of variance explained, PCA confirmed the outlier
419 positions of certain strains which displayed extreme growth behavior and the existence of two
420 groups with distinct growth behavior within the tested strains. The first group was
421 characterized by a high growth rate under optimal conditions and a reduced growth range (for

422 temperature and a_w). The second group was characterized by a lower growth rate under
423 optimal conditions and a wider growth range (for temperature and a_w).

424 Based on the distinction between technological (isolated from blue-cheese) and spoilage
425 (isolated from other environments) strains, our initial hypothesis was that spoilage strains
426 would be able to grow over a wider range of temperature and a_w which would give them an
427 adaptive advantage and that the technological strains would have been selected for their
428 higher growth rate. However, under our experimental conditions and with the 29 tested
429 strains, the present data was not sufficient to confirm this hypothesis. Regarding these
430 parameters, it can therefore be concluded that growth predictions obtained for a limited strain
431 number cannot be extrapolated to the entire *P. roqueforti* species. It is thus recommended to
432 consider the intraspecific variability of *P. roqueforti* growth response to temperature and a_w
433 for predictive mycology application (Marín et al., 2021).

434

435 In order to take into account this intraspecific variability and thus provide realistic prediction,
436 different strategies can be followed. One possible way to take this notion into account could
437 be the use of mixture of different strains to inoculate the culture medium (García et al., 2011b;
438 Romero et al., 2010). Its main advantage is to be closer to situations where more than one
439 strain of a same species may be found in the same niche (Aldars-García et al., 2018a).
440 However, García et al. (2014) indicated that the use of a mixed inoculum could be helpful to
441 estimate the mean or the median values of high number of isolates but not to account for
442 strains with marginal behavior. Furthermore, the use of strain mixture leads to worst case
443 scenario predictions because the strain with the shortest latency and highest growth rate will
444 predominate. Such predictions would finally be the safest but can lead to significant food
445 waste. Another approach could be to select one strain as a representative model on the basis
446 of specific features. If the outcomes of predictions or challenge tests are dedicated to be used

447 in a specific manufacturing site, it is obvious that the use of site-specific or recurring strains is
448 recommended. Otherwise, strains representative of a certain food process or spoilage situation
449 can be selected on the basis of current knowledge. One of the main limits of this approach is
450 the absolute requirement for a strain collection that is representative of a given fungal species,
451 which is necessary to perform an initial screening of intraspecific variability related to growth
452 behavior. As data generation is time consuming, high throughput growth measurement
453 methods such as laser nephelometry or real-time imaging are promising alternatives to study
454 large number of strains and appreciate intraspecific variability of growth in numerous
455 conditions (Aldars-García et al., 2018b). To conclude, the challenge to consider intraspecific
456 variability in predictive mycology with regards to the wide diversity of fungal spoilers
457 encountered in food would require exhaustive strain collections, but such an approach could
458 help improving accuracy of predictive models or relevance of challenge tests and should be
459 investigated for other fungal food spoilers.

460

461 **Acknowledgements**

462 This project was supported by the French Dairy Interbranch Organization (CNIEL) and the
463 French Ministry of National Education, Higher Education and Research. The authors are
464 grateful to Dr. Monika Coton for fruitful discussion and for providing the fungal strains. The
465 authors also would like to thank Maïlys Misto, Chloé Ollivier and Eva Palmieri for the
466 technical assistance in data collection.

467

468 **References**

469 Aldars-García, L., Berman, M., Ortiz, J., Ramos, A.J., Marín, S., 2018a. Probability models
470 for growth and aflatoxin B1 production as affected by intraspecies variability in
471 *Aspergillus flavus*. Food Microbiol 72, 166–175.

472 Aldars-García, L., Marín, S., Sanchis, V., Magan, N., Medina, A. 2018b. Assessment of
473 intraspecies variability in fungal growth initiation of *Aspergillus flavus* and aflatoxin B1
474 production under static and changing temperature levels using different initial conidial
475 inoculum levels. *Int J Food Microbiol* 272, 1–11.

476 Araujo, R., Rodrigues, A.G., 2004. Variability of germinative potential among pathogenic
477 species of *Aspergillus*. *J Clin Microbiol* 42, 4335–4337.

478 Augustin, J.C., Carlier, V., 2000. Mathematical modelling of the growth rate and lag time for
479 *Listeria monocytogenes*. *Int J Food Microbiol* 56, 29–51.

480 Cantor, M.D., van den Tempel, T., Hansen, T.K., Ardö, Y., 2004. Blue cheese, in: Fox, P.F.,
481 McSweeney, P.L.H., Cogan, T.M., Guinee, T.P. (Eds.), *Cheese: chemistry, physics and*
482 *microbiology*. Elsevier Academic Press, London, pp. 175–198.

483 Cuppers, H.G., Oomes, S., Brul, S., 1997. A model for the combined effects of temperature
484 and salt concentration on growth rate of food spoilage molds. *App Environ Microb* 63,
485 3764–3769.

486 Dagnas, S., Membré, J.M., 2013. Predicting and preventing mold spoilage of food products. *J*
487 *Food Prot* 76, 538–551.

488 Dantigny, P., Guilmart, A., Bensoussan, M., 2005. Basis of predictive mycology. *Int J Food*
489 *Microbiol* 100, 187–196.

490 Delhalle, L., Daube, G., Adolphe, Y., 2012. Les modèles de croissance en microbiologie
491 prévisionnelle pour la maîtrise de la sécurité des aliments (synthèse bibliographique).
492 *Biotechnol Agron Soc Environ* 16, 369–381.

493 Fontaine, K., Hymery, N., Lacroix, M.Z., Puel, S., Puel, O., Rigalma, K., Gaydou, V., Coton,
494 E., Mounier, J., 2015. Influence of intraspecific variability and abiotic factors on
495 mycotoxin production in *Penicillium roqueforti*. *Int J Food Microbiol* 215, 187–193.

496 García, D., Ramos, A.J., Sanchis, V., Marín, S., 2011a. Intraspecific variability of growth and

497 patulin production of 79 *Penicillium expansum* isolates at two temperatures. Int J Food
498 Microbiol 151, 195–200.

499 García, D., Ramos, A.J., Sanchis, V., Marín, S., 2011b. Is intraspecific variability of growth
500 and mycotoxin production dependent on environmental conditions? A study with
501 *Aspergillus carbonarius* isolates. Int J Food Microbiol 144, 432–439.

502 García, D., Ramos, A.J., Sanchis, V., Marín, S., 2009. Predicting mycotoxins in foods: a
503 review. Food Microbiol 26, 757–769.

504 García, D., Valls, J., Ramos, A.J., Sanchis, V., Marín, S., 2012. Optimising the number of
505 isolates to be used to estimate growth parameters of mycotoxigenic species. Food
506 Microbiol 32, 235–242.

507 García, D., Ramos, A. J., Sanchis, V., Marín, S., 2014. Growth parameters of *Penicillium*
508 *expansum* calculated from mixed inocula as an alternative to account for intraspecies
509 variability. Int J Food Microbiol 186, 120–124.

510 Garnier, L., Valence, F., Pawtowski, A., Auhustsinava-Galerie, L., Frotté, N., Baroncelli, R.,
511 Deniel, F., Coton, E., Mounier, J., 2017. Diversity of spoilage fungi associated with
512 various French dairy products. Int J Food Microbiol 241, 191–197.

513 Gill, C.O., Lowry, P.D., 1982. Growth at sub-zero temperatures of black spot fungi from
514 meat. J Appl Microbiol 52, 245–250.

515 Gillot, G., Jany, J.-L., Coton, M., Le Floch, G., Debaets, S., Ropars, J., López-Villavicencio,
516 M., Dupont, J., Branca, A., Giraud, T., Coton, E., 2015. Insights into *Penicillium*
517 *roqueforti* morphological and genetic diversity. PLoS ONE 10, e0129849.

518 Gillot, G., Jany, J.-L., Poirier, E., Maillard, M.-B., Debaets, S., Thierry, A., Coton, E., Coton,
519 M., 2016. Functional diversity within the *Penicillium roqueforti* species. Int J Food
520 Microbiol 241, 141–150.

521 Gougouli, M., Kalantzi, K., Beletsiotis, E., Koutsoumanis, K., 2011. Development and

522 application of predictive models for fungal growth as tools to improve quality control in
523 yogurt production. *Food Microbiol* 28, 1453–1462.

524 Gougouli, M., Koutsoumanis, K., 2013. Relation between germination and mycelium growth
525 of individual fungal spores. *Int J Food Microbiol* 161, 231–239.

526 Huet, S., Bouvier, A., Poursat, M.A., Jolivet, E., 2004. Statistical tools for nonlinear
527 regression. 2nd ed. Springer-Verlag, New York (233 pp).

528 Legan, J.D., 1993. Mould spoilage of bread: the problem and some solutions. *Int Biodeter*
529 *Biodegr* 32, 33–53.

530 Leggieri, M. C., Decontardi, S., Bertuzzi, T., Pietri, A., Battilani, P., 2017. Modeling growth
531 and toxin production of toxigenic fungi signaled in cheese under different temperature
532 and water activity regimes. *Toxins* 9, 4.

533 Leistner, L., Gorris, L.G.M., 1995. Food preservation by hurdle technology. *Trend Food Sci*
534 *Tech* 6, 41–46.

535 Marín, S., Freire, L., Femenias, A., Sant'Ana, A.S., 2021. Use of predictive modelling as tool
536 for prevention of fungal spoilage at different points of the food chain. *Curr Opin Food Sci*
537 38, 1–7

538 Morin-Sardin, S., Rigalma, K., Coroller, L., Jany, J.-L., Coton, E., 2016. Effect of
539 temperature, pH, and water activity on *Mucor* spp. growth on synthetic medium, cheese
540 analog and cheese. *Food Microbiol.* 56, 69–79.

541 Nguyen Van Long, N., Rigalma, K., Coroller, L., Dadure, R., Debaets, S., Mounier, J.,
542 Vasseur, V., 2017a. Modelling the effect of water activity reduction by sodium chloride
543 or glycerol on conidial germination and radial growth of filamentous fungi encountered in
544 dairy foods. *Food Microbiol* 68, 7–15.

545 Nguyen Van Long, N., Vasseur, V., Coroller, L., Dantigny, P., Le Panse, S., Weill, A.,
546 Mounier, J., Rigalma, K., 2017b. Temperature, water activity and pH during conidia

547 production affect the physiological state and germination time of *Penicillium* species. Int
548 J Food Microbiol 241, 151–160.

549 Perneel, M., Tambong, J.T., Adiobo, A., Floren, C., Saborío, F., Lévesque, A., Höfte, M.,
550 2006. Intraspecific variability of *Pythium myriotylum* isolated from cocoyam and other
551 host crops. Mycol Res 110, 583–593.

552 Pinon, A., Zwietering, M., Perrier, L., Membré, J.M., Leporq, B., Mettler, E., Thuault, D.,
553 Coroller, L., Stahl, V., Vialette, M., 2004. Development and validation of experimental
554 protocols for use of cardinal models for prediction of microorganism growth in food
555 products. Appl Environ Microbiol 70, 1081–1087.

556 Romero, S.M., Pinto, V.F., Patriarca, A., Vaamonde, G., 2010. Ochratoxin A production by a
557 mixed inoculum of *Aspergillus carbonarius* at different conditions of water activity and
558 temperature. Int J Food Microbiol 140, 277–281.

559 Ross, T., Olley, J., McMeekin, T.A., Ratkowsky, D.A., 2011. Some comments on Huang, L.
560 (2010). Growth kinetics of *Escherichia coli* O157: H7 in mechanically-tenderized beef.
561 Int J Food Microbiol 140: 40–48. Int J Food Microbiol 147, 78–80.

562 Rosso, L., 1995. Modélisation de microbiologie prévisionnelle : élaboration d'un nouvel outil
563 pour l'agro-alimentaire. Doctoral thesis, Université Claude Bernard, Lyon I, 190 pp.

564 Rosso, L., Lobry, J.R., Bajard, S., Flandrois, J.P., 1995. Convenient model to describe the
565 combined effects of temperature and pH on microbial growth. App Environ Microb 61,
566 610–616.

567 Saccomori, F., Wigmann, E.F., Olivier Bernandi, A., Alcano-Gonzalez, M.J. and Venturini
568 Copetti, M., 2015. Influence of storage temperature on growth of *Penicillium polonicum*
569 and *Penicillium glabrum* and potential for deterioration of frozen chicken nuggets. Int J
570 Food Microbiol 200, 1–4.

571 Santos, J.L.P., Samapundo, S., Gülay, S.M., Van Impe J., Sant'Ana, A.S., Devlieghere, F.,

572 2018. Inter- and intra- species variability in heat resistance and the effect of heat
573 treatment intensity on subsequent growth of *Byssochlamys fulva* and *Byssochlamys*
574 *nivea*. Int J Food Microbiol 279, 80–87.

575 Sautour, M., Rouget, A., Dantigny, P., Divies, C., Bensoussan, M., 2001. Prediction of
576 conidial germination of *Penicillium chrysogenum* as influenced by temperature, water
577 activity and pH. Lett Appl Microbiol 32, 131–134.

578 Stevenson, A., Hamill, P. G., O'Kane, C. J., Kminek, G., Rummel, J. D., Voytek, M. A.,
579 Dijksterhuis, J., Hallsworth, J. E. (2017). *Aspergillus penicillioides* differentiation and
580 cell division at 0.585 water activity. Environ Microbiol 19, 687–697.

581 Valík, L., Baranyi, J., Görner, F., 1999. Predicting fungal growth: the effect of water activity
582 on *Penicillium roqueforti*. Int J Food Microbiol 47, 141–146.

583 Vidal, C., Fargues, J., Lacey, L.A., 1997. Intraspecific variability of *Paecilomyces*
584 *fumosoroseus*: effect of temperature on vegetative growth. J Invertebr Pathol 70, 18–26.

585 Visconti, V., Rigalma, K., Coton, E., Dantigny, P., 2020. Impact of intraspecific variability
586 and physiological state on *Penicillium commune* inactivation by 70% ethanol. Int J Food
587 Microbiol 332, 108782

588 Walther, G., Pawłowska, J., Alastruey-Izquierdo, A., Wrzosek, M., Rodriguez-Tudela, J.L.,
589 Dolatabadi, S., Chakrabarti, A., de Hoog, G.S., 2013. DNA barcoding in Mucorales: an
590 inventory of biodiversity. Persoonia 30, 11–47.

591

592

593 **Table 1:** *Penicillium roqueforti* strains used in the present study. Strain codes used in the
594 present work. Strain number, substrate and country of origin and genetic populations (A =
595 genetic population 1, B = genetic population 2 and C = genetic population 3) are defined
596 according to Gillot et al. (2015). (*) BCCM/IHEM: Belgian Co-ordinated Collections of
597 Microorganisms, Institute of Hygiene and Epidemiology. UBOCC: Université de Bretagne
598 Occidentale Culture Collection. CBS: Centraalbureau voor Schimmcultures. DSMZ:
599 Deutsche Sammlung von Mikroorganismen und Zellkulturen. LCP: Laboratoire de
600 Cryptogamie, Paris. MUCL: Mycothèque de l'Université Catholique du Louvain. (**):
601 Hybrids but prominently assigned to population 1. (***): Hybrids between populations 2 and
602 3.

Strain code	Strain number*	Substrate of origin	Country of origin	Genetic Population
A1	BCCM/IHEM 3196	Human sputum	Belgium	1
A2	UBOCC-A-117216	Blue Stilton	United Kingdom	1
A3	UBOCC-A-117220	Fourme d'Ambert	France	1
A4	UBOCC-A-117221	Bleu Basque	France	1**
A5	UBOCC-A-117214	Blue mold cheese	New-Zealand	1**
B1	UBOCC-A-111178	Air (Dairy industry)	France	2
B2	CBS 112579	Sulphite liquor	Canada	2
B3	DSMZ 1999	Beef meat	Switzerland	2
B4	MUCL 35036	Wood in process of drying in the open air (<i>Quercus</i> sp.)	France	2
B5	CBS 498.73	Apple	Russia	2
B6	UBOCC-A-109090	Apricot (preparation)	France	2
B7	LCP03969	Fruit compote	France	2
B8	UBOCC-A-111033	Corn silage	France	2
B9	UBOCC-A-117222	Bleu des Causses	France	2
B10	CBS 221.30	Roquefort	USA	2
B11	UBOCC-A-111172	Air (dairy industry)	France	2
B12	UBOCC-A-111170	Surface (dairy industry)	France	2
B13	CBS 304.97	Mozzarella	Denmark	2
B14	MUCL 18048	Cork	Belgium	2
B15	UBOCC-A-117123	Blue mold cheese	New-Zealand	2
B16	UBOCC-A-117127	Roquefort	France	2
B17	UBOCC-A-113020	Roquefort	France	2
B18	UBOCC-A-117124	Blue mold cheese	Argentina	2
B19	UBOCC-A-110052	Olive brine	France	2
B20	UBOCC-A-113022	Roquefort	France	2
C1	UBOCC-A-113008	Blue mold cheese	Latvia	3

C2	UBOCC-A-117213	Bleu du Vercors - Sassenage	France	3
C3	UBOCC-A-101449	Fruit (preparation)	France	3***
C4	UBOCC-A-113014	Gorgonzola	Italy	3

603

604

605 **Table 2:** Cardinal temperatures and a_w of 29 *P. roqueforti* including minimal (T_{min} and a_{wmin}), optimal (T_{opt} and a_{wopt}) and maximal (T_{max}) levels
606 for latency and reciprocal of latency for radial growth under optimal conditions (λ^{-1}_{opt}). These parameters were estimated by fitting Eq. 2 to
607 reciprocal of latency for radial growth (λ). The accuracy of the model is characterized by means of root mean square error (RMSE) and
608 determination coefficient (r^2).

Strain	T_{min} (°C)	T_{opt} (°C)	T_{max} (°C)	a_{wmin} (-)	a_{wopt} (-)	λ^{-1}_{opt} (d ⁻¹)	r^2 (-)	RMSE (d ⁻¹)
A1	-11.5 ± 0.4	35.3 ± 0.3	35.3 ± 0.3	0.801 ± 0.006	0.988 ± 0.000	1.11 ± 0.01	0.975 - 0.979	0.048 - 0.052
A2	-12.4 ± 2.6	29.5 ± 3.5	31.2 ± 1.3	0.788 ± 0.009	0.991 ± 0.003	0.74 ± 0.11	0.801 - 0.931	0.065 - 0.121
A3	-12.8 ± 0.4	32.7 ± 1.4	32.7 ± 1.4	0.810 ± 0.002	0.982 ± 0.004	0.91 ± 0.06	0.932 - 0.959	0.059 - 0.078
A4	-10.6 ± 1.5	29.1 ± 1.3	30.0 ± 0.0	0.752 ± 0.022	0.984 ± 0.000	0.84 ± 0.07	0.976 - 0.985	0.035 - 0.043
A5	-10.1 ± 1.2	29.7 ± 0.5	30.0 ± 0.0	0.807 ± 0.006	0.983 ± 0.001	0.88 ± 0.04	0.954 - 0.990	0.028 - 0.062
B1	-7.9 ± 0.6	30.0 ± 0.0	30.0 ± 0.0	0.748 ± 0.011	0.978 ± 0.001	1.12 ± 0.05	0.855 - 0.902	0.112 - 0.131
B2	-6.8 ± 1.7	25.2 ± 1.1	32.0 ± 0.6	0.707 ± 0.044	0.993 ± 0.001	0.78 ± 0.02	0.737 - 0.801	0.127 - 0.152
B3	-10.2 ± 0.9	30.5 ± 0.9	30.6 ± 0.9	0.778 ± 0.008	0.980 ± 0.001	0.85 ± 0.01	0.901 - 0.907	0.092 - 0.094
B4	-4.0 ± 1.9	22.7 ± 1.8	29.9 ± 2.1	0.763 ± 0.018	0.986 ± 0.006	0.77 ± 0.05	0.924 - 0.984	0.040 - 0.092
B5	-7.1 ± 3.4	27.0 ± 1.1	33.3 ± 1.8	0.678 ± 0.078	0.998 ± 0.002	0.84 ± 0.07	0.863 - 0.937	0.072 - 0.106
B6	-6.8 ± 0.4	29.2 ± 0.4	30.2 ± 0.2	0.764 ± 0.004	0.984 ± 0.001	1.17 ± 0.02	0.959 - 0.970	0.065 - 0.077
B7	-10.6 ± 0.3	30.4 ± 0.7	30.4 ± 0.7	0.778 ± 0.003	0.976 ± 0.001	0.97 ± 0.03	0.939 - 0.954	0.064 - 0.070
B8	-4.5 ± 1.2	22.7 ± 0.7	33.1 ± 0.8	0.754 ± 0.006	0.989 ± 0.003	0.80 ± 0.03	0.926 - 0.972	0.042 - 0.072
B9	-7.0 ± 1.5	24.9 ± 0.8	31.2 ± 0.4	0.747 ± 0.003	0.992 ± 0.002	0.69 ± 0.01	0.703 - 0.822	0.112 - 0.161
B10	-12.4 ± 4.1	27.2 ± 3.4	30.4 ± 0.5	0.744 ± 0.045	0.991 ± 0.001	0.70 ± 0.09	0.783 - 0.946	0.061 - 0.113
B11	-2.1 ± 0.2	21.5 ± 0.5	28.9 ± 0.2	0.758 ± 0.020	0.986 ± 0.002	0.97 ± 0.07	0.806 - 0.942	0.084 - 0.157
B12	-8.0 ± 0.6	27.0 ± 0.0	27.0 ± 0.0	0.769 ± 0.009	0.984 ± 0.000	1.05 ± 0.04	0.891 - 0.940	0.082 - 0.109
B13	-8.4 ± 0.8	30.0 ± 0.0	30.0 ± 0.0	0.788 ± 0.005	0.984 ± 0.000	1.11 ± 0.01	0.958 - 0.965	0.066 - 0.070
B14	-2.2 ± 0.9	22.4 ± 0.4	33.2 ± 0.3	0.779 ± 0.019	0.989 ± 0.003	0.91 ± 0.06	0.854 - 0.936	0.085 - 0.136
B15	-11.3 ± 1.8	27.8 ± 1.6	31.4 ± 1.2	0.792 ± 0.009	0.992 ± 0.001	0.83 ± 0.05	0.865 - 0.937	0.074 - 0.111

B16	-7.0 ± 1.7	28.4 ± 1.5	30.6 ± 0.8	0.757 ± 0.008	0.995 ± 0.002	0.92 ± 0.07	0.901 - 0.950	0.071 - 0.096
B17	-9.0 ± 1.3	26.3 ± 1.1	31.1 ± 0.5	0.693 ± 0.029	0.993 ± 0.001	0.73 ± 0.04	0.757 - 0.965	0.052 - 0.137
B18	-5.2 ± 4.5	25.2 ± 3.3	31.7 ± 1.2	0.804 ± 0.004	0.986 ± 0.001	0.96 ± 0.07	0.840 - 0.886	0.113 - 0.136
B19	-10.9 ± 0.4	30.0 ± 0.0	30.0 ± 0.0	0.646 ± 0.076	0.977 ± 0.001	0.96 ± 0.02	0.828 - 0.954	0.061 - 0.127
B20	-2.9 ± 0.4	22.2 ± 0.3	33.4 ± 0.2	0.777 ± 0.014	0.989 ± 0.001	0.84 ± 0.02	0.818 - 0.880	0.106 - 0.134
C1	-8.8 ± 0.2	27.0 ± 0.0	27.0 ± 0.0	0.785 ± 0.009	0.988 ± 0.001	0.97 ± 0.02	0.946 - 0.980	0.045 - 0.075
C2	-10.9 ± 0.6	27.0 ± 0.0	27.0 ± 0.0	0.754 ± 0.006	0.989 ± 0.001	0.82 ± 0.03	0.906 - 0.940	0.068 - 0.089
C3	-7.9 ± 1.2	24.6 ± 0.7	28.8 ± 1.2	0.707 ± 0.007	0.991 ± 0.002	0.83 ± 0.02	0.870 - 0.921	0.080 - 0.107
C4	-12.0 ± 0.6	29.2 ± 0.6	30.0 ± 0.0	0.776 ± 0.011	0.990 ± 0.003	0.87 ± 0.02	0.952 - 0.985	0.033 - 0.060

609

610

611 **Table 3:** Cardinal temperatures and a_w of 29 *P. roqueforti* including minimal (T_{min} and a_{wmin}), optimal (T_{opt} and a_{wopt}) and maximal (T_{max}) levels
612 for radial growth rate and radial growth rate under optimal conditions (μ_{opt}). These parameters were estimated by fitting Eq. 2 to radial growth
613 rate (μ). The accuracy of the model is characterized by means of root mean square error (RMSE) and determination coefficient (r^2).

Strain	T_{min} (°C)	T_{opt} (°C)	T_{max} (°C)	a_{wmin} (-)	a_{wopt} (-)	μ_{opt} (mm.d ⁻¹)	r^2 (-)	RMSE (mm.d ⁻¹)
A1	-15.3 ± 1.0	24.2 ± 0.2	30.1 ± 0.0	0.844 ± 0.002	0.984 ± 0.001	5.84 ± 0.02	0.955 - 0.964	0.169 - 0.193
A2	-15.9 ± 1.0	27.8 ± 0.1	30.0 ± 0.0	0.839 ± 0.005	0.989 ± 0.000	6.08 ± 0.09	0.963 - 0.971	0.156 - 0.187
A3	-14.6 ± 0.6	23.3 ± 0.1	30.2 ± 0.0	0.832 ± 0.009	0.982 ± 0.002	5.60 ± 0.10	0.963 - 0.982	0.112 - 0.151
A4	-13.6 ± 1.2	23.7 ± 0.2	30.1 ± 0.0	0.833 ± 0.000	0.981 ± 0.000	6.07 ± 0.02	0.987 - 0.992	0.079 - 0.097
A5	-9.4 ± 1.0	24.8 ± 0.1	30.1 ± 0.0	0.831 ± 0.012	0.985 ± 0.001	6.57 ± 0.16	0.973 - 0.992	0.090 - 0.161
B1	-12.2 ± 0.9	23.0 ± 0.2	30.3 ± 0.0	0.841 ± 0.001	1.007 ± 0.001	6.57 ± 0.18	0.948 - 0.980	0.127 - 0.219
B2	-15.4 ± 1.0	24.1 ± 0.4	30.2 ± 0.0	0.852 ± 0.023	0.998 ± 0.006	5.92 ± 0.07	0.953 - 0.977	0.140 - 0.202
B3	-14.9 ± 2.3	25.2 ± 1.0	30.2 ± 0.1	0.833 ± 0.001	0.988 ± 0.001	7.01 ± 0.13	0.959 - 0.984	0.119 - 0.184
B4	-18.0 ± 3.3	27.2 ± 2.8	30.1 ± 0.1	0.825 ± 0.003	0.989 ± 0.002	6.08 ± 0.40	0.966 - 0.985	0.105 - 0.160
B5	-27.2 ± 8.1	28.5 ± 3.0	30.1 ± 0.1	0.824 ± 0.002	0.982 ± 0.000	4.97 ± 0.09	0.936 - 0.975	0.104 - 0.186
B6	-21.7 ± 2.9	24.1 ± 0.6	30.2 ± 0.1	0.816 ± 0.004	0.983 ± 0.001	3.78 ± 0.11	0.969 - 0.980	0.084 - 0.111
B7	-13.9 ± 0.9	23.5 ± 0.4	30.3 ± 0.0	0.829 ± 0.002	1.001 ± 0.001	6.00 ± 0.05	0.943 - 0.957	0.175 - 0.209
B8	-18.5 ± 1.0	26.9 ± 0.1	30.1 ± 0.0	0.816 ± 0.003	0.981 ± 0.002	4.21 ± 0.04	0.969 - 0.983	0.083 - 0.112
B9	-16.4 ± 1.5	24.3 ± 0.6	30.2 ± 0.0	0.813 ± 0.011	1.003 ± 0.012	4.64 ± 0.20	0.967 - 0.990	0.070 - 0.127
B10	-9.1 ± 2.1	24.7 ± 2.0	30.2 ± 0.2	0.855 ± 0.017	1.001 ± 0.002	6.67 ± 0.40	0.924 - 0.980	0.149 - 0.264
B11	-21.9 ± 3.0	28.4 ± 1.2	30.0 ± 0.0	0.810 ± 0.003	1.006 ± 0.001	4.24 ± 0.17	0.886 - 0.942	0.158 - 0.199
B12	-18.7 ± 2.1	26.0 ± 0.8	30.2 ± 0.1	0.806 ± 0.004	1.009 ± 0.001	5.09 ± 0.27	0.944 - 0.977	0.106 - 0.155
B13	-18.0 ± 4.9	25.1 ± 0.4	30.2 ± 0.0	0.808 ± 0.004	1.012 ± 0.002	5.80 ± 0.11	0.966 - 0.980	0.111 - 0.138
B14	-35.4 ± 3.9	27.5 ± 0.5	29.1 ± 1.7	0.792 ± 0.028	1.032 ± 0.006	3.34 ± 0.27	0.808 - 0.824	0.268 - 0.334
B15	-10.2 ± 0.3	26.3 ± 0.2	30.1 ± 0.0	0.838 ± 0.004	0.988 ± 0.001	5.44 ± 0.05	0.966 - 0.991	0.081 - 0.159
B16	-23.3 ± 3.9	24.5 ± 0.5	30.1 ± 0.0	0.753 ± 0.012	0.983 ± 0.002	5.39 ± 0.06	0.897 - 0.971	0.109 - 0.219
B17	-8.8 ± 0.5	24.9 ± 0.3	30.3 ± 0.0	0.837 ± 0.001	1.003 ± 0.002	6.81 ± 0.32	0.966 - 0.973	0.161 - 0.176

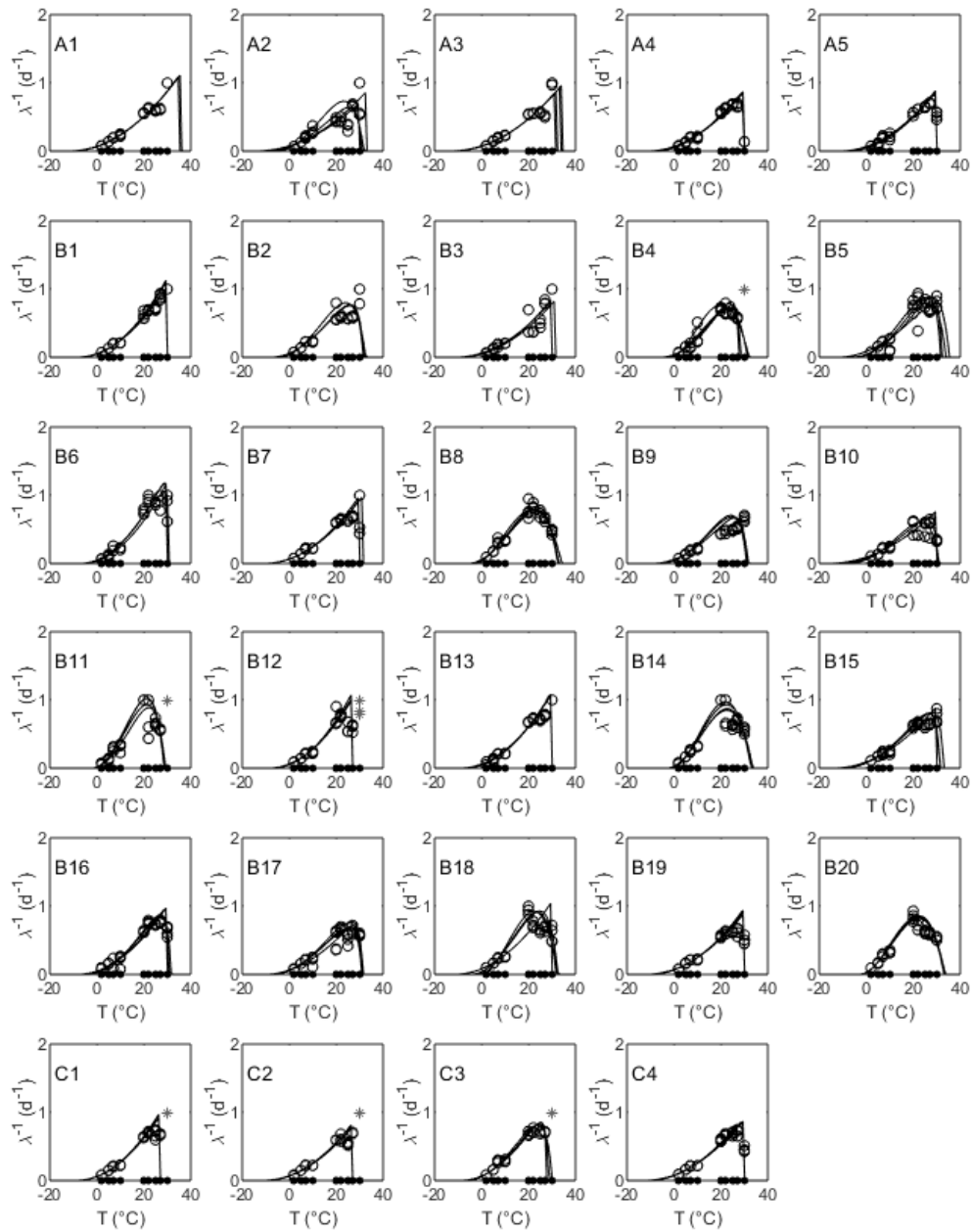
B18	-25.1 ± 0.5	25.9 ± 0.1	30.2 ± 0.0	0.842 ± 0.002	0.981 ± 0.001	4.32 ± 0.07	0.936 - 0.956	0.148 - 0.185
B19	-25.1 ± 1.7	22.5 ± 0.5	30.3 ± 0.0	0.807 ± 0.001	0.987 ± 0.001	4.83 ± 0.09	0.947 - 0.956	0.146 - 0.150
B20	-25.7 ± 1.7	26.6 ± 0.4	30.1 ± 0.0	0.837 ± 0.002	0.985 ± 0.001	4.60 ± 0.07	0.928 - 0.952	0.159 - 0.203
C1	-17.1 ± 0.5	23.1 ± 0.3	30.2 ± 0.0	0.838 ± 0.003	0.986 ± 0.001	4.82 ± 0.02	0.963 - 0.971	0.134 - 0.154
C2	-18.7 ± 1.0	23.9 ± 0.3	30.1 ± 0.0	0.834 ± 0.001	0.982 ± 0.001	4.98 ± 0.07	0.977 - 0.987	0.090 - 0.117
C3	-15.4 ± 0.8	25.5 ± 0.3	30.2 ± 0.0	0.836 ± 0.000	0.983 ± 0.001	5.42 ± 0.09	0.967 - 0.977	0.122 - 0.145
C4	-12.3 ± 1.5	23.1 ± 0.7	30.3 ± 0.1	0.826 ± 0.002	0.982 ± 0.001	5.55 ± 0.07	0.981 - 0.986	0.092 - 0.107

614

615

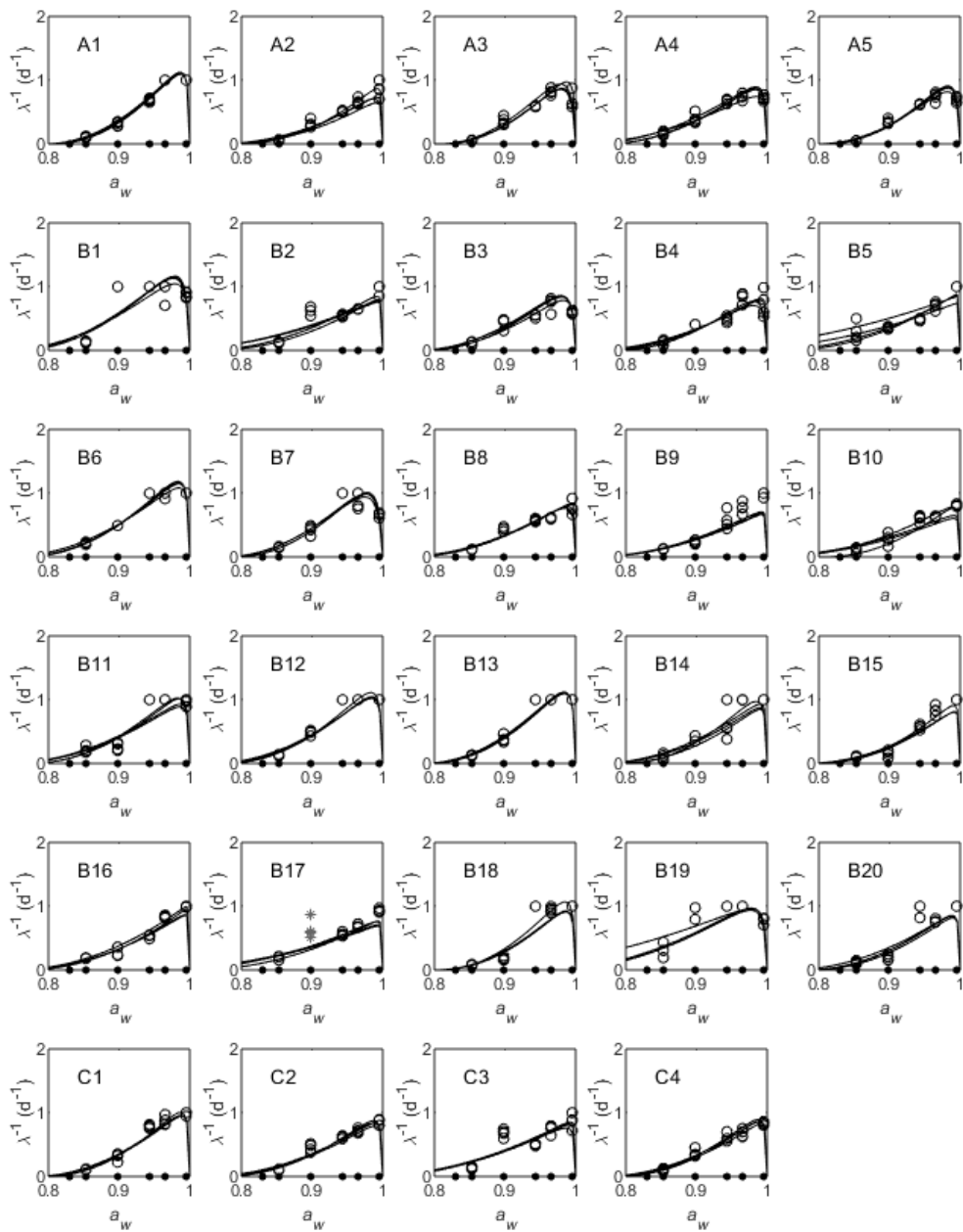
616

617 **Fig. 1:** Secondary models describing the effect of temperature ($^{\circ}\text{C}$) on reciprocal of latency
618 (λ^{-1} , d^{-1}) for radial growth of 29 *Penicillium roqueforti* strains (strain number indicated on
619 upper left corner of each graph). Eq. 2 (solid line) was fitted to observed parameters (open
620 circles). Tested temperatures are shown as solid circles. Data discarded for secondary
621 modelling are shown as asterisks. Four independent biological replicates are displayed.

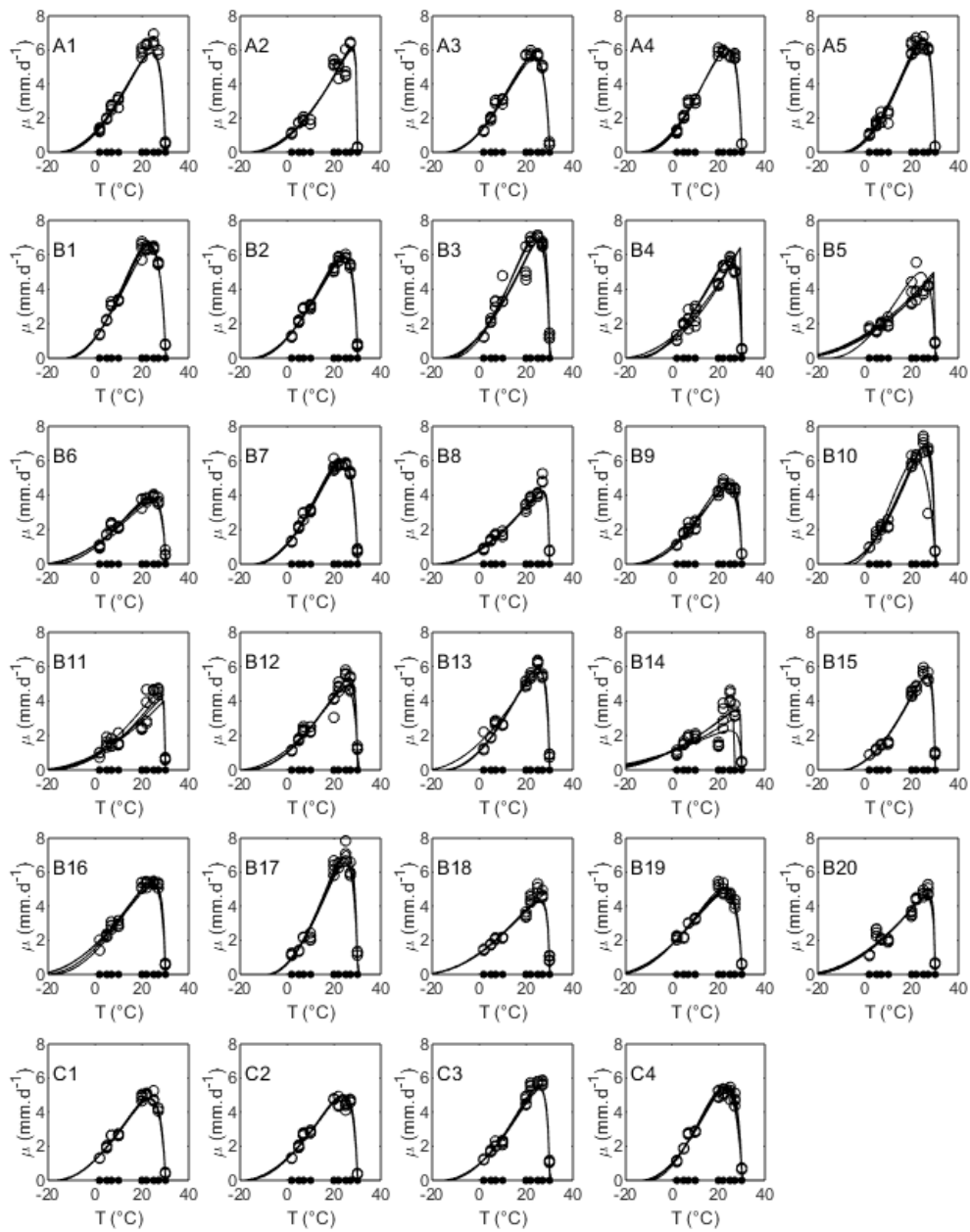


622

623 **Fig. 2:** Secondary models describing the effect of a_w (-) on reciprocal of latency (λ^{-1} , d⁻¹) for
 624 radial growth of 29 *Penicillium roqueforti* strains (strain number indicated on upper left
 625 corner of each graph). Eq. 2 (solid line) was fitted to observed parameters (open circles).
 626 Tested a_w levels are shown as solid circles. Data discarded for secondary modelling are shown
 627 as asterisks. Four independent biological replicates are displayed.

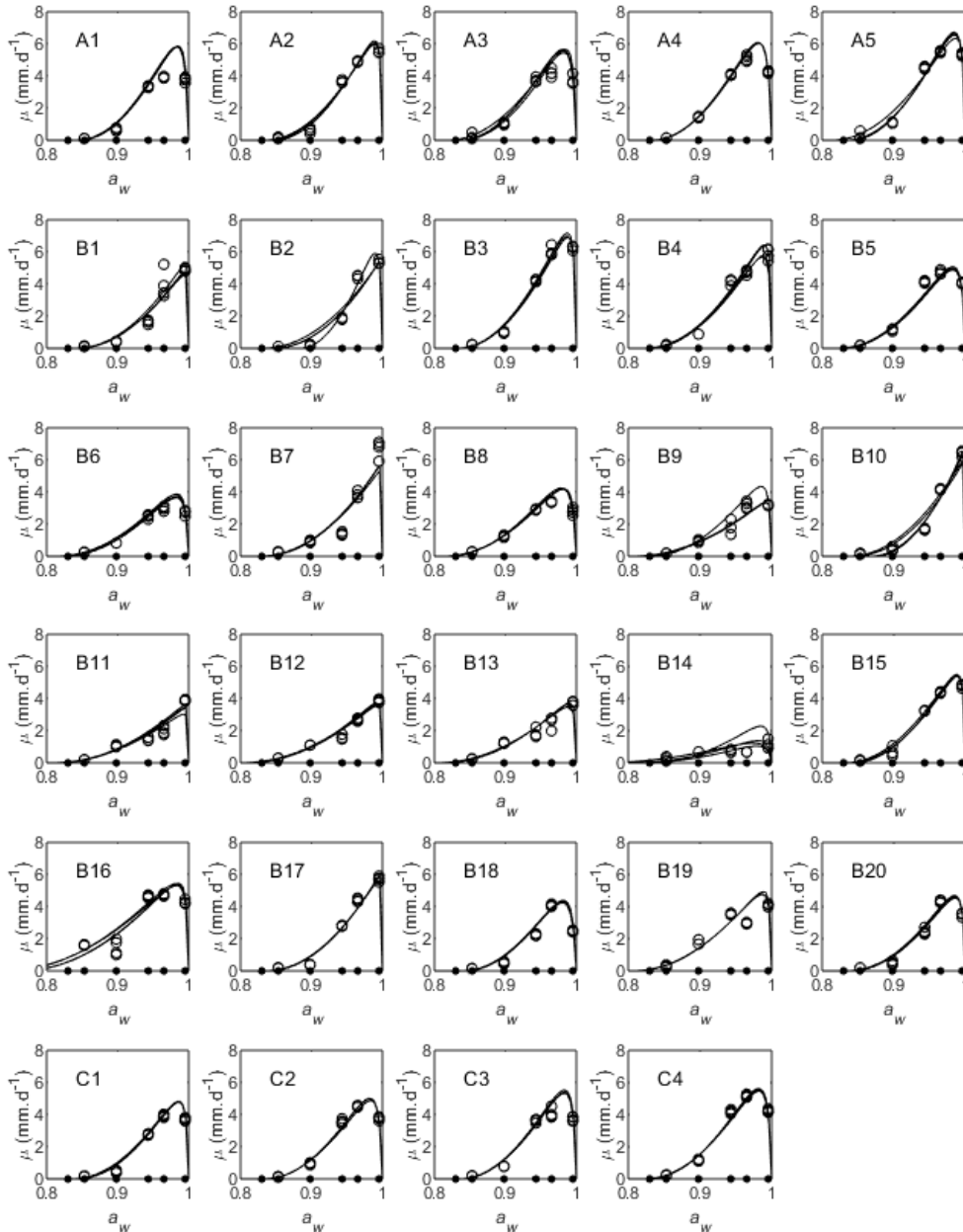


629 **Fig. 3:** Secondary models obtained to describe the effect of temperature ($^{\circ}\text{C}$) on the radial
 630 growth rate (μ , $\text{mm}\cdot\text{d}^{-1}$) of 29 *Penicillium roqueforti* strains (strain number indicated on upper
 631 left corner of each graph). Eq. 2 (solid line) was fitted to observed parameter (open circles).
 632 Tested temperatures are shown as solid circles. Four independent biological replicates are
 633 displayed.



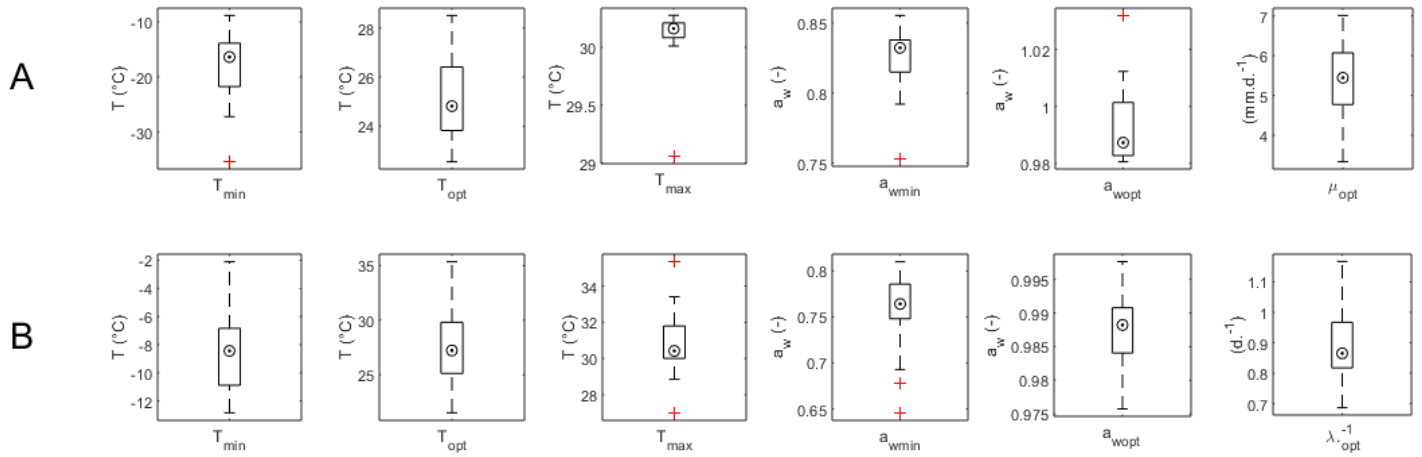
634

635 **Fig. 4:** Secondary models obtained to describe the effect of a_w (-) on the radial growth rate (μ ,
 636 mm.d⁻¹) of 29 *Penicillium roqueforti* strains (strain number indicated on upper left corner of
 637 each graph). Eq. 2 (solid line) was fitted to observed parameter (open circles). Tested a_w
 638 levels are shown as solid circles. Four independent biological replicates are displayed.



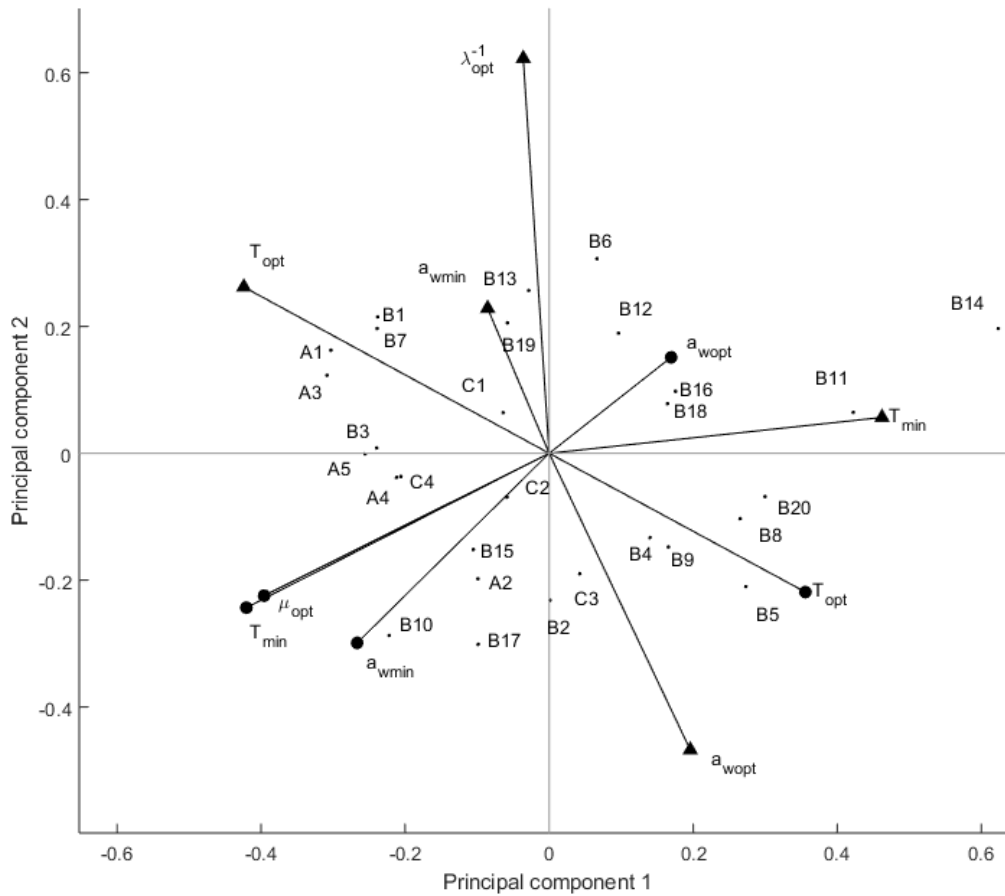
639

640 **Fig. 5:** Box plot figures representing the variability of T_{min} , T_{opt} , T_{max} , a_{wmin} , a_{wopt} , λ^{-1}_{opt} and
 641 μ_{opt} parameters. A: figures for latency for growth. B: figures for radial growth rate. Solid box
 642 represents the range between 25th and 75th percentiles. Empty circle with black dot represents
 643 the median value. The whiskers extend to the minimum and maximum values not considered
 644 outliers. Red crosses represent outlier data.



645

646 **Fig. 6:** Principal component analysis of the cardinal temperatures, a_w and associated
 647 parameters estimated for the 29 tested *P. roqueforti* strains. Component 1 and 2 correspond to
 648 36.80 % and 20.74 % of the total variance respectively. Variables related to latency for radial
 649 growth (λ): $\blacktriangle T_{min}$, $\blacktriangle T_{opt}$, $\blacktriangle a_{wmin}$, $\blacktriangle a_{wopt}$, $\blacktriangle \lambda^{-1}_{opt}$, variables related to radial growth rate
 650 (μ): $\bullet T_{min}$, $\bullet T_{opt}$, $\bullet a_{wmin}$, $\bullet a_{wopt}$, $\bullet \mu_{opt}$. Individuals represented by dots are the 29 tested *P.*
 651 *roqueforti* strains belonging to 3 genetically differentiated populations (A = genetic
 652 population 1, B = genetic population 2 and C = genetic population 3).



653

